




Pressure dependence of antiferromagnetic and superconducting phases in $U_2Rh_{1-x}Pt_xC_2$

Sangyun Lee ^{1,2,*}, Yongkang Luo,^{3,†} F. Ronning,^{3,4} N. Wakeham ^{3,‡}, E. D. Bauer,³ Duk Y. Kim,²
J. D. Thompson ^{3,§} and Tuson Park^{1,||}

¹Center for Quantum Materials and Superconductivity (CQMS) and Department of Physics, Sungkyunkwan University, Suwon 16419, South Korea

²Center for Integrated Nanostructure Physics (CINAP), Institute for Basic Science (IBS), Sungkyunkwan University, Suwon, 16419, South Korea

³Materials Physics and Applications-Quantum, Los Alamos National Laboratory, Los Alamos, New Mexico 87545, USA

⁴Institute for Materials Science, Los Alamos National Laboratory, Los Alamos, New Mexico 87545, USA



(Received 10 March 2020; revised 21 June 2020; accepted 22 June 2020; published 13 July 2020)

We report temperature (T)- and pressure (P)-dependent resistivity measurements on the isostructural compounds $U_2Rh_{1-x}Pt_xC_2$ ($x = 0, 0.5$, and 0.9) from which we construct a T - P - x phase diagram. Compounds with $x = 0$ and $x = 0.5$ are antiferromagnets below 22.1 and 9.4 K, respectively, and their Néel temperature (T_N) decreases under applied pressure. For $x = 0$, the critical pressure P_c required to suppress T_N to zero temperature is projected to be about 8.8 GPa, but P_c for $x = 0.5$ is between 1.6 and 2.1 GPa. At atmospheric pressure, increasing Pt concentration in $U_2Rh_{(1-x)}Pt_xC_2$ tunes magnetic transition temperatures to zero at a critical value of $x_c \approx 0.7$, and, consequently, we surmise the existence of a quantum-phase boundary in the $P-x$ plane at $T = 0$ K that extends from ($P = 0, x = x_c$) to ($P_c \approx 8.8$ GPa, $x = 0$). For $x = 0.9$, superconductivity appears at $T_c = 1.09$ K, which decreases at a rate of ≈ -1 K/GPa that is nearly twice that found for U_2PtC_2 whose T_c is 1.47 K. Together, these results indicate that domes of magnetism and superconductivity formed with T - P - x variations are detached and that the two broken symmetries are independent of each other. Fluctuations in average composition produce rare regions that play an important role in determining physical properties of materials with noninteger x .

DOI: [10.1103/PhysRevB.102.035124](https://doi.org/10.1103/PhysRevB.102.035124)

I. INTRODUCTION

Historically, the relationship between magnetism and superconductivity in uranium-based compounds was attributed to the distance between nearest U atoms, d_{U-U} [1]. From plotting superconducting (T_c) and magnetic (T_N) transition temperatures as a function of d_{U-U} , Hill noticed that superconductivity appeared predominantly at $d_{U-U} < 3.4$ Å and magnetism at $d_{U-U} > 3.6$ Å and suggested that the separation in ground states might be understood if the overlap of $5f$ wave functions at smaller d_{U-U} promoted itineracy of the $5f$ electrons and f -band formation that supports phonon-mediated superconductivity, but at larger d_{U-U} the $5f$ wave functions were localized, favoring magnetic order. This concept, though useful at the time, failed to account for subsequently discovered U-based superconductors whose U-U spacing far

exceeded the Hill limit [2]. These anomalous superconductors with large U-U separation now are understood to be part of a family of heavy-fermion superconductors in which spin fluctuations produce an attractive interaction that promotes Cooper pairing with finite angular momentum and nodal structure of the superconducting gap [3,4]. Instead of only d_{U-U} determining the fate of $5f$ electrons and the ground state as in Hill's interpretation, hybridization between atomiclike f and ligand electrons plays the dominant role in these heavy-fermion superconductors where even in a single compound magnetic order and superconductivity can coexist and both involve uranium's $5f$ electrons [5,6].

The body-centered-tetragonal series $U_2Rh_{1-x}Pt_xC_2$ is particularly interesting for studying the interplay of magnetism and superconductivity in relation to U-U spacing and hybridization. U_2RhC_2 , with its U-U spacing of ~ 3.46 Å [7], should be on the border of superconductivity by Hill's criterion, but instead it orders antiferromagnetically at 22 K [8]. In contrast, U_2PtC_2 has $d_{U-U} \approx 3.52$ Å, which implies by the same reasoning that it should be close to magnetic order, but it is superconducting below 1.47 K [9]. Both end compounds of the series have a modestly enhanced Sommerfeld coefficient of specific heat ($\gamma \approx 120$ ($x = 0$) and 75 ($x = 1$) mJ/mol U K² [8,10]), consistent with the presence of electron-electron interactions deduced from band structure calculations [11]. Here, the quoted γ for $x = 0$ is determined from a linear fit of specific heat C divided by temperature T (C/T) versus T^2 above T_N , which should reflect intrinsic electronic correlations in U_2RhC_2 ; whereas, the literature

*Present address: Materials Physics and Applications-Quantum, Los Alamos National Laboratory, Los Alamos, New Mexico 87545, USA.

†Present address: Wuhan National High Magnetic Field Center, Huazhong University of Science and Technology, Wuhan 430074, Hubei, China.

‡Present address: NASA Goddard Space Flight Center, Greenbelt, MD, 20771, USA and CRESST II – University of Maryland, Baltimore County, MD, 21250, USA.

§Corresponding author: jdt@lanl.gov

||Corresponding author: tp8701@skku.edu

value of ~ 80 mJ/mol U K² is determined deep in the magnetically order state [8]. A partial reduction of γ by magnetic order is typical of correlated U-based antiferromagnets [2]. As x increases from 0, the Néel temperature reaches at maximum near $x = 0.1$ ($T_N = 22.9$ K) before decreasing monotonically to $T_N = 0$ K near $x = 0.7$, where γ diverges and exceeds 200 mJ/mol U K² at 0.38 K [8]. These observations imply the presence of a quantum-critical point (QCP) near $x_c = 0.7$ at atmospheric pressure. With further increasing x , superconductivity appears (above 0.38 K) for $x \geq 0.9$ [8], and for $x = 1$, experiments suggested that the superconductivity may be nodal. For example, the superconducting penetration depth increases approximately linearly and the nuclear spin-lattice relaxation rate $1/T_1$ decreases as a power law with decreasing temperature below T_c [12,13], both contrary to expectations for a fully gapped superconductor. Further, the Knight shift remains unchanged from above to below T_c , which, along with $1/T_1 \propto T^2$, is consistent with nodal spin-triplet superconductivity [13].

Across the $U_2Rh_{1-x}Pt_xC_2$ series, the U-U spacing and unit cell volume increase monotonically with increasing x [8], which suggests that evolution of ground states is not controlled simply by wave function overlap, i.e., d_{U-U} . Replacing Rh with Pt not only introduces disorder but also adds nominally one d electron/ x , both of which could contribute to the ground-state evolution. Application of hydrostatic pressure, in contrast, does not introduce additional disorder or change the nominal electron count but reduces the cell volume. If reducing the cell volume were the only effect of applied pressure, we might expect, in light of ground-state changes with x , that pressure decreases the Néel temperature of U_2RhC_2 ($x = 0$), increases T_N of magnetically ordered compounds with $x \geq 0.1$, and induces magnetism in the superconducting materials. As we will show from pressure-dependent resistivity measurements on polycrystalline samples with $x = 0, 0.5$, and 0.9 , only the first possibility is realized experimentally. Further, from these measurements and the known pressure dependence of T_c for $x = 0$ [14], we will demonstrate that superconductivity in Pt-rich compounds is unrelated to antiferromagnetism found at the Rh-rich end.

II. EXPERIMENTAL DETAILS

Samples were taken from the same arc-melted and annealed buttons used in Ref. [8]. Briefly, buttons were prepared by arc melting constituents with a molar ratio U:Pt:Rh:C of 2: 1.1 x : 1.1(1- x): 2.2, flipped and remelted several times and finally wrapped in Ta foil and annealed in an evacuated quartz tube for 2 months at 1050 °C. The crystal structure and actual doping concentration were determined via x-ray diffraction (XRD) and energy-dispersive x-ray spectroscopy measurements. XRD confirmed the Na_2HgO_2 structure type and the presence of paramagnetic UC, UC_2 , Rh or Pt at a total level of <10%. Electrical resistivity measurements on bar-shaped samples cut from the button were made with the conventional four-probe technique under hydrostatic pressure conditions. Platinum wires were attached to the samples via spot welding, and silver epoxy was additionally applied to secure the contacts. A hybrid piston-type cell and a mixture of silicon liquid and glycerol-water (60/40) as the pressure-

transmitting medium were used to generate hydrostatic pressures to 2.6 GPa [15]. The superconducting transition temperature of Pb was used to determine the pressure inside the cell [16].

III. RESULTS

Figure 1(a) shows the ground-state phase diagram of $U_2Rh_{1-x}Pt_xC_2$ as a function of the Pt concentration x , where T_N and T_c are denoted by stars and circles, respectively [8]. The three concentrations, $x = 0, 0.5$, and 0.9 that are the subject of this study, are marked by arrows in Fig. 1(a), and their electrical resistivity (ρ) at the ambient pressure is plotted as a function of temperature, in Fig. 1(b). The resistivity of U_2PtC_2 ($x = 1$) is included for reference. Overall, these results agree well with a previous report [8], as do values of T_c and T_N , the latter in our case being defined from the minimum in the first temperature derivative of the resistivity, $d\rho/dT$ indicated by arrows in Fig. 1(c). The signature of T_N in $d\rho/dT$ reflects a weak chromiumlike anomaly in $\rho(T)$, suggesting spin-density wave order. This suggestion is consistent with a small polycrystalline-averaged saturated moment ($\sim 0.3 \mu_B/U$) below T_N that is much reduced from the high-temperature effective moment ($2.8 \mu_B/U$) and with entropy below T_N of only $\sim 0.4R \ln 2$ (where R is the gas constant) [8]. Both are expected if $5f$ electrons is hybridized at least to some extent with ligand electrons to give the $5f$'s simultaneously atomic and itinerant characters.

Qualitatively, the resistivity of each material shows a similar temperature dependence and the resistivity ratio $\rho(300\text{ K})/\rho(2\text{ K})$ is modestly large for the end members, 10.3 for $x = 0$ and 18 for $x = 1$ [8]. The smaller resistivity ratio for $x = 0$ may be attributed partially to the opening of a spin-density wave gap that removes some itinerant carriers below T_N and to the presence of magnon scattering in the ordered state at finite temperature. The magnetically ordered state or at least scattering processes in it, however, may be more complex. In the Supplemental Material we discuss fits of the resistivity below T_N to various functional forms used in the literature to describe transport in the ordered states of antiferromagnets and ferromagnets [17]. Possibly because the magnetic order is complex, none of these functions gives a compelling description of the resistivity of $x = 0$ or $x = 0.5$ materials at atmospheric or elevated pressure. We also discuss in the Supplemental Material the temperature dependence of resistivity in the paramagnetic state of samples with $x = 0, 0.5, 0.9$, and 1.0 [17].

Turning now to results of pressure measurements, we first consider U_2RhC_2 whose resistivity at various pressures up to 2.6 GPa is plotted in Fig. 2(a). The overall resistivity decreases with increasing pressure, and the weak Cr-like anomaly near 22 K at 1 bar broadens and moves to lower temperatures. With d_{U-U} of U_2RhC_2 close to Hill's criterion for f -electron itinerancy, the general pressure-induced decrease in resistivity can be understood qualitatively as arising from a combination of increasing overlap of f -wave functions and hybridization of f - and conduction-electron states that together broaden a narrow band near the Fermi energy and decrease spin scattering. The decrease in T_N with increasing pressure is more obvious in plots of $d\rho/dT$ shown in Fig. 2(b). As seen in Fig. 2(c), T_N

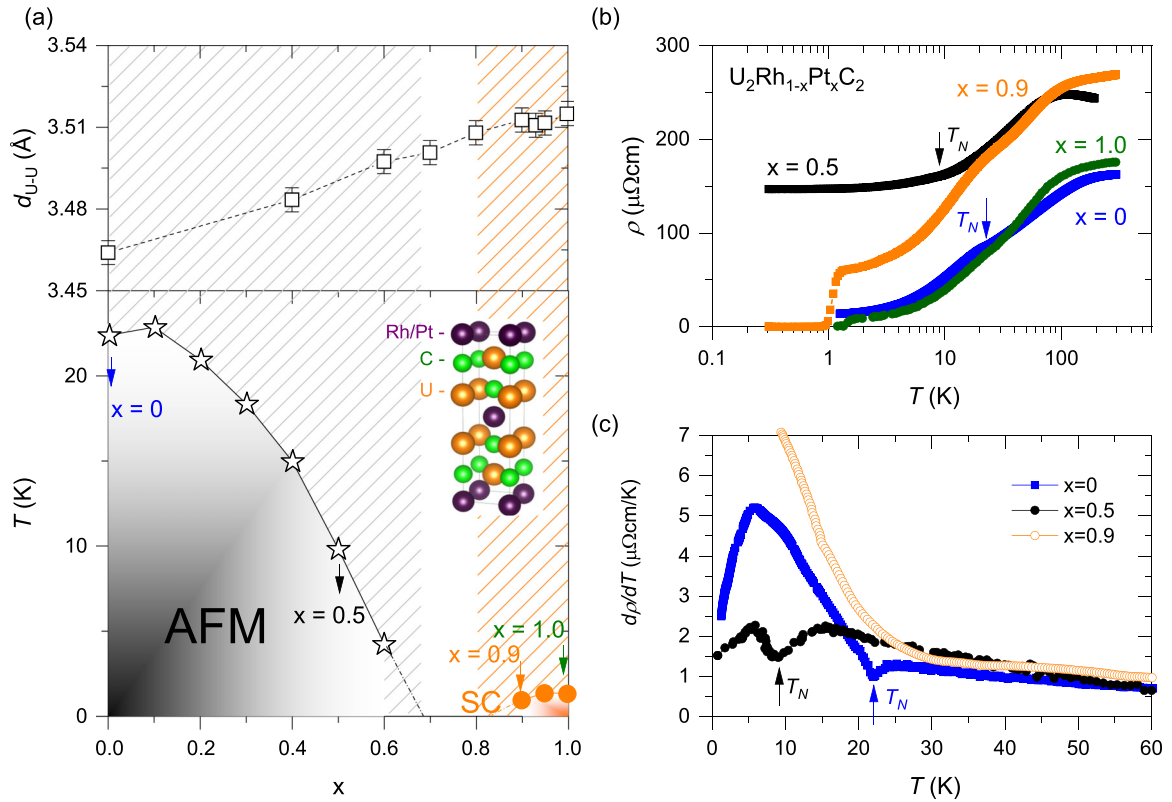


FIG. 1. Response of $\text{U}_2\text{Rh}_{1-x}\text{Pt}_x\text{C}_2$ at atmospheric pressure to changing x . (a) Upper panel: Variation of d_{U-U} with increasing x [8]. d_{U-U} corresponds to the in-plane lattice parameter of the tetragonal structure. Variation of the tetragonal anisotropy as a function of x is given in the Supplemental Material [17]. Lower panel: Phase diagram of $\text{U}_2\text{Rh}_{1-x}\text{Pt}_x\text{C}_2$ adapted from Ref. [8]. Stars represent antiferromagnetic (AFM) transition temperatures and circles give superconducting (SC) transition temperatures. The blue, black, orange, and green arrows indicate values of $x = 0, 0.5, 0.9$, and 1 , respectively. The inset shows the crystal structure of $\text{U}_2\text{Rh}_{1-x}\text{Pt}_x\text{C}_2$. (b) Resistivity as a function of temperature on the semilogarithmic scales for $x = 0$ (blue), $x = 0.5$ (black), $x = 0.9$ (orange), and $x = 1.0$ (green symbols). Resistivity of $x = 1.0$ is taken from [8]. (c) Temperature derivative of the resistivity. Colors correspond to those in (b). The solid arrows indicate T_N at $x = 0$ and $x = 0.5$.

decreases approximately linearly at a rate of -2.52 K/GPa. This relatively slow rate of decrease of T_N with pressure follows the trend of T_N to decrease weakly with decreasing cell volume for $x \leq 0.1$. Assuming this rate of decrease of T_N with pressure remains constant at higher pressures, then T_N extrapolates to zero temperature at a critical pressure P_c of about 8.8 GPa.

As shown in Fig. 1(b), the residual resistivity for $x = 0.5$ is by far the largest among samples studied, which is expected from maximal quench-disorder scattering at the middle of the substitutional series [18]; however, from the pressure dependence shown in Fig. 3(a), ρ_0 clearly is not dominated by simple potential scattering arising from quench disorder. Because pressure does not introduce additional chemical or site disorder, the large ($\sim 70 \mu\Omega\text{cm}$) decrease in ρ_0 between 1 bar and 2.1 GPa must be a consequence of suppressed scattering by spin/charge fluctuations that are not removed by the development of antiferromagnetic order. Indeed, the existence of low-energy excitations below T_N is evident in ambient-pressure specific heat measurements that find C/T increasing in the ordered state to over 150 mJ/mol U K^2 , well above the value of C/T just above T_N [8]. The origin of these excitations is not obvious, but proximity to a quantum-critical point at $x_c(P=0) \sim 0.7$ is a potential source of excitations which we consider further in the Discussion section.

The large residual resistivity in $\text{U}_2\text{Rh}_{0.5}\text{Pt}_{0.5}\text{C}_2$ obscures an obvious signature for T_N in $\rho(T)$, but it becomes clearer from the minimum in $d\rho/dT$ that is marked in Fig. 3(b). From these data T_N decreases approximately linearly from 9.4 K at ambient pressure to 2.5 K at 1.6 GPa, and at 2.1 GPa, there is no detectable signature in $d\rho/dT$ for a magnetic transition above 0.35 K, signaling the presence of an antiferromagnetic quantum-critical point between 1.6 and 2.1 GPa. The rate of decrease, $dT_N/dP = -4.3$ K/GPa, is 1.7 times larger and gives a nearly four times larger magnetic Gruneisen parameter $\partial \ln T_N / \partial \ln P$ compared to those in U_2RhC_2 . The latter in particular is consistent with the closer proximity of $\text{U}_2\text{Rh}_{0.5}\text{Pt}_{0.5}\text{C}_2$ to a quantum-critical point at 1 bar [19]. Both the negative dT_N/dP and Gruneisen parameter are completely opposite to the trend of T_N with cell volume for $x \geq 0.1$ in the substitutional series.

Because $\text{U}_2\text{Rh}_{0.5}\text{Pt}_{0.5}\text{C}_2$ already is relatively near a magnetic-nonmagnetic boundary at 1 bar and only modest pressure is sufficient to tune its Néel temperature to zero, we expect quantum-critical fluctuations to be important even in the ordered state. Generically, these fluctuations give rise to a non-Fermi-liquid power-law temperature dependence of resistivity with exponent less than 2 near a quantum-critical point [20], and as seen in Fig. 3(c), $\rho(T) = \rho_0 + A_n T^n$ semi-quantitatively describes the data over an extended temperature

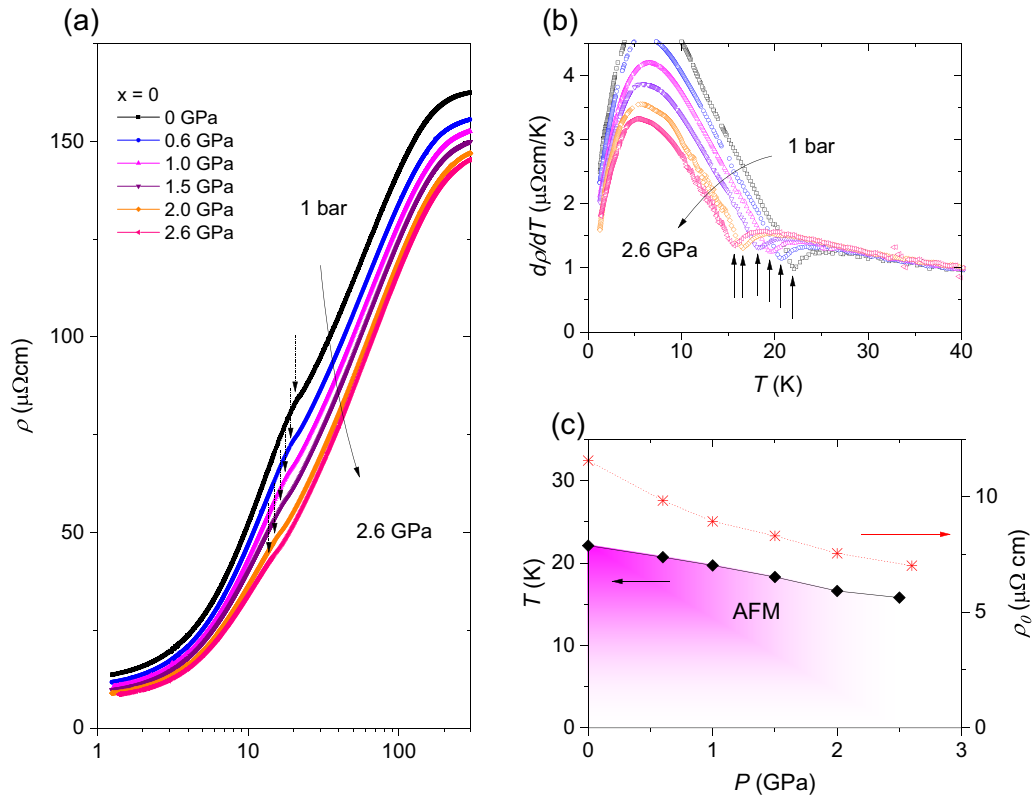


FIG. 2. Pressure dependence of the resistivity of U_2RhC_2 . (a) Resistivity at indicated pressures as a function of temperature on a semilogarithmic scale. Black dashed arrows mark the shoulders near T_N . (b) Temperature derivative of the resistivity at pressures to 2.6 GPa. Colors correspond to those in (a). Black solid arrows mark T_N . (c) Pressure dependence of T_N (solid diamonds) and residual resistivity (stars).

range. Parameters A_n and n are plotted in Fig. 3(d) as a function of pressure, and the trends are typical of those of a magnetic system tuned to a quantum-critical point; however, in systems that are relatively defect-free, the residual resistivity typically is a maximum at the QCP, which clearly contrasts with results in Fig. 3(a) where ρ_0 decreases throughout the entire pressure range that includes the projected critical pressure.

At the Pt-rich end of the series, superconductivity develops below $T_c = 1.09$ K in the $x = 0.9$ sample as shown by resistivity measurements in Fig. 4(a). In this material and in contrast to results on $\text{U}_2\text{Rh}_{0.5}\text{Pt}_{0.5}\text{C}_2$, there is relatively little pressure dependence on the magnitude of the low-temperature resistivity and no evidence from specific heat or magnetic susceptibility for proximity to a quantum-critical point [8]. Nevertheless, the resistivity above T_c has a non-Fermi-liquid temperature dependence at 1 bar [Fig. 4(b)] and evolves with pressure toward a T^2 Fermi-liquid behavior, as shown in Fig. 4(c). This evolution is accompanied by a decrease in T_c that falls below 0.30 K for $P \geq 1.1$ GPa. If superconductivity is spin-triplet as proposed for U_2PtC_2 [13], it is surprising that it survives at all in $\text{U}_2\text{Rh}_{0.1}\text{Pt}_{0.9}\text{C}_2$, which has a 1-bar residual resistivity of $\sim 55 \mu\Omega\text{cm}$ that is at least a factor of five larger (and more than a factor of 20 times larger in our samples) than in U_2PtC_2 [8], let alone with a T_c that is still $\approx 75\%$ of that in U_2PtC_2 .

Previous specific heat measurements on $\text{U}_2\text{Rh}_{0.1}\text{Pt}_{0.9}\text{C}_2$ confirm that its superconductivity is bulk but find a jump

$\Delta C/C$ at T_c that is less than half that of the $x = 1$ compound and a large residual C/T in the zero-temperature limit [8]. If the coupling strength does not decrease dramatically with 10% Rh substitution, then the reduced jump in C suggests a corresponding reduction in the superconducting volume fraction. This suggestion is consistent with the broad superconducting transition of $x = 0.9$ in a magnetic field that is shown in Fig. 4(d). With criteria of 90% and 10% of the normal state resistivity to define the transition width, the so-defined critical fields are 5.3 and 2.6 T, respectively, and it is difficult to argue against the existence of significant heterogeneity. Whether this heterogeneity translates to a roughly 50% volume fraction of a superconducting phase in zero field remains to be determined, but it is consistent with a less than full superconducting volume fraction.

The temperature-pressure-substitution (T - P - x) phase diagram in Fig. 5 summarizes our principal results that find a dome of antiferromagnetic order bounded at $T = 0$ by a line of critical points spanning ($P = 0$, $x = x_c \leq 0.7$) and ($P \sim 8.8$ GPa, $x = 0$), which is separate from a dome of superconductivity at the Pt-rich end of the phase diagram. More specifically, (1) $x = 0$: Pressure slowly decreases the Néel temperature of U_2RhC_2 as expected from increased $5f$ -ligand hybridization and from the ambient-pressure response of T_N to decreasing cell volume of $x \leq 0.1$ $\text{U}_2\text{Rh}_{1-x}\text{Pt}_x\text{C}_2$ materials. A linear extrapolation of $T_N(P)$ to $T_N = 0$ gives a critical pressure $P_c \sim 8.8$ GPa. (2) $x = 0.5$: The Néel temperature of $\text{U}_2\text{Rh}_{0.5}\text{Pt}_{0.5}\text{C}_2$ is less than half that of U_2RhC_2 and is

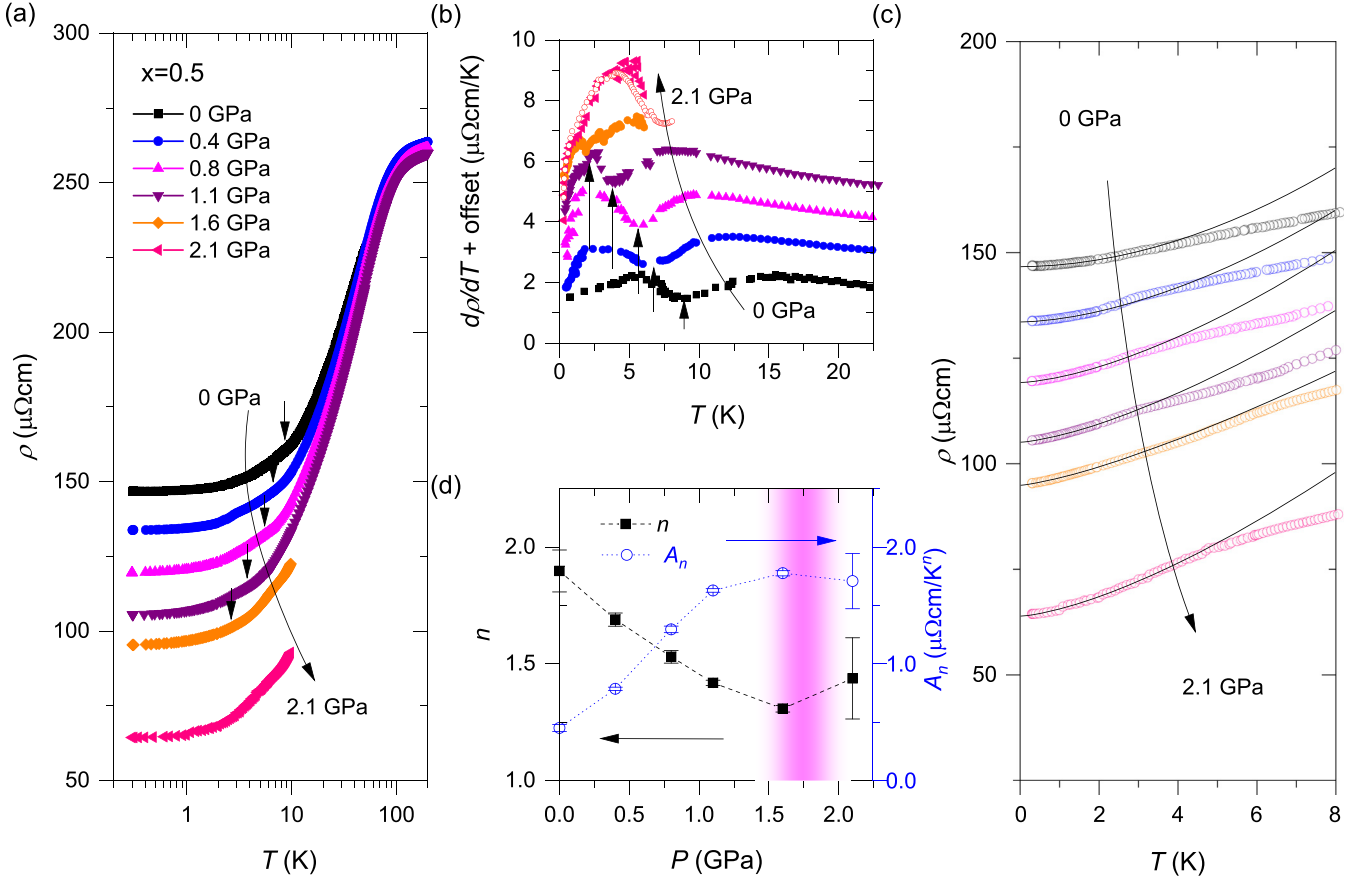


FIG. 3. Pressure dependence of $\text{U}_2\text{Rh}_{0.5}\text{Pt}_{0.5}\text{C}_2$. (a) Electrical resistivity of $\text{U}_2\text{Rh}_{0.5}\text{Pt}_{0.5}\text{C}_2$ at various pressures to 2.1 GPa as a function of temperature on a semilogarithmic scale. Arrows mark T_N determined from temperature derivatives. (b) Temperature derivative of the resistivity. Colors correspond to those used in (a) and arrows denote T_N . For clarity, curves are offset vertically. (c) Low-temperature resistivity (open symbols) and least-squares fits (solid curves) to $\rho(T) = \rho_0 + A_n T^n$ at various pressures. Fits are made over the temperature range 0.3 to 2 K, and the fit function is plotted to higher temperatures for purposes of illustration. (d) Pressure dependence of parameters extracted from fits shown in (c). Black squares and blue circles denote the exponent n and T coefficient A_n , respectively. The shaded vertical region around 1.7 GPa denotes a range of possible pressures where the transition of bulk antiferromagnetic orders reaches $T = 0$. The variation of these fitting parameters with pressure is robust, independently of reasonable temperature ranges for the fits. For example, fitting data over intervals [0.3, 1], [0.3, 2], [0.3, 3], and [0.3, 4] gives similar trends with applied pressure, though absolute values of fitting parameters change somewhat. A fuller discussion of the resistivity is given in the Supplemental Material [17].

suppressed at a higher rate, giving $T_N = 0$ at a critical pressure $1.6 \leq P \leq 2.1$ GPa. The negative pressure derivative of T_N is completely opposite to the ambient-pressure positive response of T_N to decreasing cell volume for $0.1 \leq x \leq x_c \approx 0.7$. The residual resistivity of $x = 0.5$ is by far the highest in the series and decreases substantially and monotonically with pressures to 2.1 GPa. The resistivity below T_N is described best by a power-law temperature dependence that takes a non-Fermi-liquid form as the critical pressure is approached. (3) $x = 0.9$: $\text{U}_2\text{Rh}_{0.1}\text{Pt}_{0.9}\text{C}_2$ develops superconductivity below 1.09 K out of a highly resistive ($\sim 55 \mu\Omega\text{cm}$) and weakly pressure-dependent normal state. The superconductivity, whose T_c decreases rapidly with pressure, may be present in less than the full sample volume. (4) Finally, we note that, though electronic correlations may be somewhat more significant near the $x = 0$ end of the series, they are relevant for all members, and that disorder on the ligand site could nontrivially influence physical properties of samples with noninteger x .

IV. DISCUSSION

We take the end compounds, $x = 0$ and 1, as representative of pressure responses in the absence of ligand-site disorder. The slow, monotonic decline of T_N with decreasing cell volume in U_2RhC_2 is characteristic of pressure-enhanced $5f$ -ligand hybridization in a material that is relatively far from a QCP but whose atomiclike $5f$ wave functions already have mixed somewhat with ligand states at $P = 0$. UPtGa_5 is another example of this physics. Its antiferromagnetic ordering temperature, ordered moment, and Sommerfeld coefficient are quite similar to those of U_2RhC_2 as are the sign and magnitude of dT_N/dP and critical pressure of UPtGa_5 [21]. The larger unit cell volume and U-U spacing in U_2PtC_2 lead to strong ferromagnetic correlations evident in its normal-state Korringa response and Wilson ratio greater than 2 [13]. Such ferromagnetic correlations arise among band electrons when electron-electron repulsion is sufficiently strong, a condition favored in narrow-band materials [22]. Increasing hybridization and correspondingly the electronic bandwidth with applied

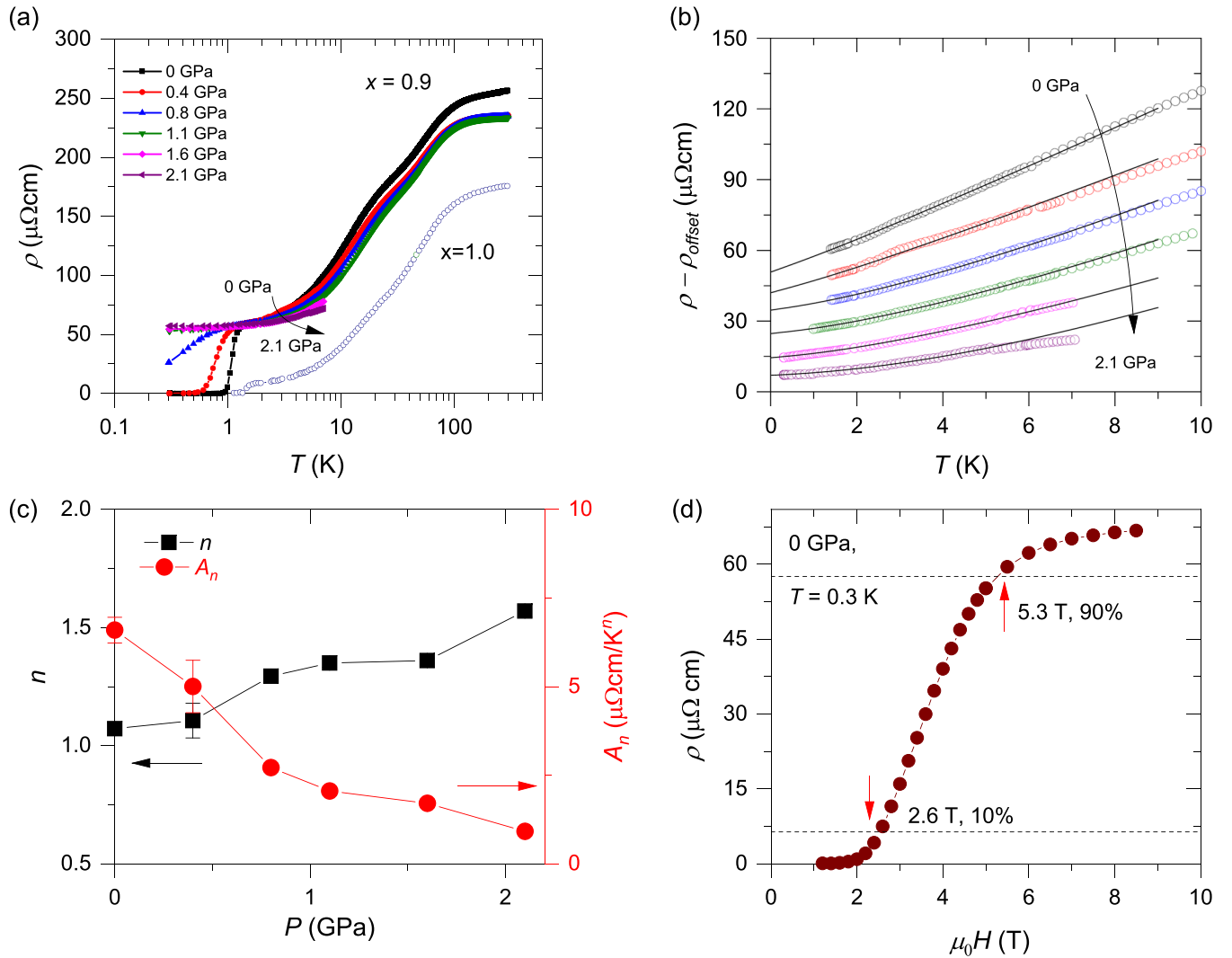


FIG. 4. Pressure response of $\text{U}_2\text{Rh}_{0.1}\text{Pt}_{0.9}\text{C}_2$. (a) Temperature dependence of the electrical resistivity of $\text{U}_2\text{Rh}_{0.1}\text{Pt}_{0.9}\text{C}_2$ ($x = 0.9$) at various pressures up to 2.1 GPa. The electrical resistivity of U_2PtC_2 at ambient pressure [8] is included for comparison. (b) Temperature dependence of the low- T resistivity (open symbols) and least-squares fits (solid curves) to the power-law form $\rho(T) = \rho_0 + A_n T^n$. Fits are made in the temperature range from 5 K down to either T_c (if superconductivity is present) or to 0.3 K and are plotted to higher temperatures for the purpose of illustration. For clarity, each curve is displaced by a constant ρ_{offset} relative to $\rho(T)$ at 0 GPa. (c) Pressure dependence of parameters extracted from fits. Black squares and red circles denote the exponent n and T coefficient A_n , respectively. Error in determining the fit parameters may be somewhat larger at low pressures because the lower limit of the fitting range is restricted by the onset of superconductivity. (d) Electrical resistivity of the $x = 0.9$ sample at 0.3 K and ambient pressure as a function of the magnetic field. Arrows mark the temperatures at which the resistivity is 90% and 10% of the normal-state value.

pressure reduces the importance of ferromagnetic correlations. In other U-base superconductors believed to be spin-triplet, applied pressure suppresses T_c if pressure moves them away from a $T = 0$ ferromagnetic instability [23]. This likely is the same reason why T_c of U_2PtC_2 decreases with pressure [14], as shown in Fig. 5. Namely, applied pressure tunes U_2PtC_2 away from proximity to a $T = 0$ ferromagnetic instability by promoting hybridization, broadening the correlated band and reducing ferromagnetic correlations.

Replacing 10% of Pt with Rh reduces T_c to 1.09 K from 1.47 K in U_2PtC_2 and applied pressure leads to a further decrease in T_c without any signature of AFM order. Like pressure, the smaller cell volume of $\text{U}_2\text{Rh}_{0.1}\text{Pt}_{0.9}\text{C}_2$ is expected to reduce T_c by weakening ferromagnetic correlations,

but this substitution also removes 0.1 electron/formula unit. Iridium substitution for Pt in $\text{U}_2\text{Ir}_{1-x}\text{Pt}_x\text{C}_2$ has a similar but somewhat stronger effect on T_c [24] and as with 10% Rh substitution, Ir removes 0.1 electron/formula unit, reduces the unit cell volume, and increases the residual resistivity very much as in $\text{U}_2\text{Rh}_{0.1}\text{Pt}_{0.9}\text{C}_2$ [25]. At a qualitative level, there is no significant difference between Rh and Ir substitutions, so Rh is not acting in any particularly anomalous way. Both types of substitutions, however, introduce ligand-site disorder while keeping the U-lattice intact. Even with a purely random distribution of Rh/Pt, for any given average value of x statistically there will be regions that are richer in one element than in the other, evoking the role of rare-regions and Griffiths-phase physics [26]. We have, then, at a minimum

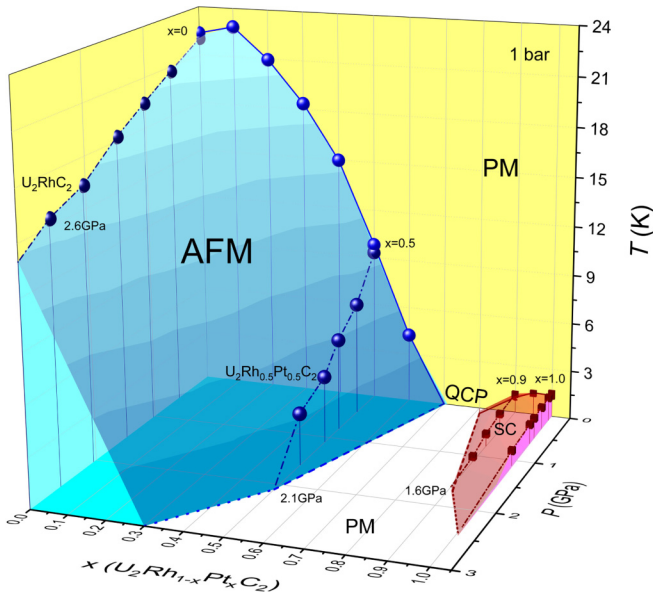


FIG. 5. Temperature-pressure-substitution (T - P - x) phase diagram of $U_2Rh_{(1-x)}Pt_xC_2$. The dependences of T_c and T_N on x at the ambient pressure are from Ref. [8], and the pressure dependence of T_c at $x = 1.0$ is from Ref. [14]. A dome of antiferromagnetism (AFM) is bounded at $T = 0$ by a projected line of quantum critical points (QCP) and is well-separated from superconductivity (SC) at the Pt-rich end of the diagram. PM denotes a paramagnetic phase with no long-range order.

in the Rh/Pt substitution series a very complex situation: a change in unit cell volume, global average hybridization, strength of ferromagnetic correlations, and nominal electron count as well as a nonuniform distribution of composition.

To varying extents, each of these must play a role in determining the physical properties of $U_2Rh_{0.1}Pt_{0.9}C_2$. If superconductivity in this $x = 0.9$ compound also is spin-triplet, as implied by its large critical field that exceeds the Pauli limit and as proposed for U_2PtC_2 [13], then the very existence of triplet superconductivity that develops out of such a highly resistive ($\sim 55 \mu\Omega \text{ cm}$) normal state implicates heterogeneity. A nonuniform distribution of Pt/Rh produces clusters that are rich in either Rh or Pt. Ten percent Rh is well below the site percolation limit of $\sim 24.5\%$ for a body-centered-tetragonal lattice on which the Rh/Pt atom sites [27], and so there is no continuous path of Rh atoms. But, rare regions rich in Rh are inevitable and favor the development of local antiferromagnetic correlations. If their spatial extent reaches a few lattice constants, they will form local patches of antiferromagnetic order with Néel temperatures ranging from near zero and up to $\sim 22 \text{ K}$ depending on composition. Quantum fluctuations of these rare regions, especially those with T_N close to zero, lead to pronounced non-Fermi-liquid properties [28,29]. Similarly, there must be locally Pt-rich region, which, if larger than a coherence length of $\sim 50 \text{ \AA}$ [13], will be superconducting with composition-dependent T_c 's ranging from zero to 1.46 K . Scattering within and between heterogeneous regions with such a broad range of characters will lead to a large residual resistivity as well as a proliferation of excitations and states ungapped by superconductivity that reasonably account for a

reduced 1-bar specific heat jump at T_c , whereas superconductivity, possibly spin-triplet, survives in the dominantly large regions with $x \approx 0.1$ where the electronic mean-free path is comparable to or longer than a coherence length. Applying pressure does not change the static heterogeneity, so the residual resistivity should depend only weakly on pressure as found experimentally. It will, however, preferentially suppress scattering by quantum fluctuations of rare Rh-rich regions that are most magnetically susceptible, i.e., locally have a large magnetic Gruneisen response, and move the system toward a Fermi-liquid state, which is evident in Fig. 4(c).

The manifestation of randomness and rare regions, characteristic of a Griffiths phase, is clear in results for the $x = 0.5$ compound. If potential scattering dominates, the residual resistivity of a random solution of Rh/Pt should be a maximum when the atomic concentration of components is equal [18]. This is the case with $U_2Rh_{0.5}Pt_{0.5}C_2$, but its residual resistivity at atmospheric pressure is far larger than expected from quench disorder alone and strongly pressure dependent. At this average composition, there is a roughly equal distribution of Rh and Pt rare regions, each with their own characteristics and local hybridization of $5f$ and band electrons that in principle span the phase diagram of Fig. 1. The system is maximally disordered, giving rise to the very large residual resistivity. As with the $x = 0.1$ material, pressure preferentially suppresses scattering by quantum fluctuations of rare regions that locally have a large magnetic Gruneisen response and moves the system toward a Fermi-liquid state. A Fermi-liquid state, however, cannot be reached because the average response, reflected in $T_N(P)$, is tuned to a QCP where quantum fluctuations of the average magnetic order parameter as well as quantum Griffiths fluctuations become pronounced [29]. This competition accounts qualitatively for pressure variations in non-Fermi-liquid parameters shown in Fig. 3(d) and the absence of a maximum in residual resistivity expected at a pressure-tuned QCP.

In light of this discussion, we also can understand the origin of a diverging C/T and non-Fermi-liquid temperature dependence of the resistivity at $x_c \approx 0.7$. The composition-tuned QCP develops not because the global average hybridization or direct $5f$ wave function overlap have increased sufficiently to suppress long-range order but instead because of critical slowing down of quantum-driven rare-region temporal fluctuations. In principle, long-range Ruderman-Kittel-Kasuya-Yosida (RKKY) interactions between rare regions favors formation of a cluster glass state at low temperatures in the Griffiths phase around x_c [30], a possibility that deserves further exploration.

The qualitative picture that emerges from our measurements is that rare regions play an important role in determining physical properties for materials with noninteger x . A statistical distribution of Rh and Pt around an average x creates local variations in $5f$ -conduction electron hybridization and spin-spin interactions that have an influence disproportionate to their small volume fraction and become particularly important near a phase transition. Though singular contributions to thermodynamic and transport properties have been modeled in the context of a quantum Griffiths phase [29,31], direct comparison to our experimental results is difficult because essential relevant parameters of models are unknown, e.g.,

effective dimensionality of the rare regions, importance of long-range (RKKY) interactions, or even the universality class of the antiferromagnetic order. Transport measurements that we present are particularly challenging because singular contributions from rare regions are mixed with parallel and series conduction paths through material that is dominantly of the average composition. Nevertheless, the concepts of Griffiths physics provide a qualitative but consistent and logical framework for interpreting our observations, as we have described. To enable at least a semiquantitative comparison to models, it would be useful to measure thermodynamic properties, such as specific heat and magnetic susceptibility, over closely spaced variations of x in $U_2Rh_{1-x}Pt_xC_2$ and for comparison in $U_2Rh_{1-x}M_xC_2$, where M is a transition metal isoelectronic with Rh, as a function of pressure for values of x around a composition-tuned quantum critical point, to determine the nature of magnetic order in $x = 0$, and to determine the distribution and spatial extent of rare regions. At the same time, it would be useful to extend models to account for rare regions with qualitatively different spin-spin correlations, e.g., antiferromagnetic and ferromagnetic.

V. CONCLUSION

To summarize, the primary role of U-U spacing is to tune the relative importance of antiferromagnetic and ferromagnetic correlations as x increases from 0 to 1, respectively, while having relatively little influence on the extent of $5f$ -conduction-band mixing in the end compounds whose U-U spacing differ by more than 10%. Aside from U_2RhC_2 , the effect of pressure on the ground state is exactly opposite that expected based on trends with either U-U-spacing or cell volume. As expected, however, applied pressure reduces

magnetic correlations in the end members by modestly increasing $5f$ -band hybridization. Away from the end compounds, properties depend on a complex interplay of effects, with randomness and rare regions, characteristic of a Griffiths phase, dominating the T - P - x phase diagram. From our results and discussion of them, we conclude that superconductivity at the Pt-rich end of the diagram is independent of antiferromagnetism at the Rh-rich end, more specifically that quantum fluctuations of the average antiferromagnetic order are irrelevant for producing superconductivity. This leaves open the possibility that superconductivity may be spin-triplet, as proposed from nuclear magnetic resonance studies on U_2PtC_2 [13], and we reason how this superconductivity can persist relatively undiminished even in the $x = 0.9$ material that has a large residual resistivity. The nature of antiferromagnetic order and the search for a possible cluster-glass state around $x = 0.7$ are interesting problems left for future work.

ACKNOWLEDGMENTS

We thank N. Ni for her contributions to the preparation of samples. Work at Sungkyunkwan University was supported by a NRF grant funded by the Ministry of Science, and ICT (Grant No. 2012R1A3A2048816). Work at Los Alamos was performed under the auspices of the US Department of Energy, Office of Science, Division of Materials Science and Engineering. All authors discussed the results and commented on the manuscript. S.L. and Y.L. performed transport measurements under the pressure. S.L. analyzed the corresponding data. F.R. and N.W. characterized samples. E.B. provided samples. S.L., D.K., J.D.T., and T.P. wrote the manuscript with input from all authors.

-
- [1] H. H. Hill, in *Plutonium 1970 and Other Actinides*, edited by W. N. Miner (The Metallurgical Society of the AIME, New York, 1970), p. 2.
 - [2] H. R. Ott and Z. Fisk, in *Handbook on the Physics and Chemistry of Actinides*, edited by A. J. Freeman and G. H. Lander (North Holland, Amsterdam, 1987), p. 85.
 - [3] M. Sigrist and K. Ueda, *Rev. Mod. Phys.* **63**, 239 (1991).
 - [4] D. J. Scalapino, *Rev. Mod. Phys.* **84**, 1383 (2012).
 - [5] C. Geibel *et al.*, *Z. Phys. B* **84**, 1 (1991).
 - [6] J. Flouquet, *Prog. Low Temp. Phys.* **15**, 139 (2005).
 - [7] H. Holleck, *J. Nucl. Mater.* **28**, 339 (1968).
 - [8] N. Wakeham, Ni Ni, E. D. Bauer, J. D. Thompson, E. Tegmeier, and F. Ronning, *Phys. Rev. B* **91**, 024408 (2015).
 - [9] B. T. Matthias, C. W. Chu, E. Corenzwit, and D. Wohlleben, *Proc. Natl. Acad. Sci. USA* **64**, 459 (1969).
 - [10] G. P. Meisner, A. L. Giorgi, A. C. Lawson, G. R. Stewart, J. O. Willis, M. S. Wire, and J. L. Smith, *Phys. Rev. Lett.* **53**, 1829 (1984).
 - [11] F. Ronning and J.-X. Zhu, *J. Phys. Conf. Ser.* **592**, 012037 (2015).
 - [12] W. D. Wu, A. Keren, L. P. Le, G. M. Luke, B. J. Sternlieb, Y. J. Uemura, N. Sato, T. Komatsubara, and G. P. Meisner, *Hyperfine Interact.* **85**, 425 (1994).
 - [13] A. M. Mounce, H. Yasuoka, G. Koutroulakis, N. Ni, E. D. Bauer, F. Ronning, and J. D. Thompson, *Phys. Rev. Lett.* **114**, 127001 (2015).
 - [14] J. D. Thompson and G. P. Meisner, *Physica B* **130**, 168 (1985).
 - [15] I. R. Walker, *Rev. Sci. Instrum.* **70**, 3402 (1999).
 - [16] A. Eiling and J. S. Schilling, *J. Phys. F* **11**, 623 (1981).
 - [17] See Supplemental Material at <http://link.aps.org/supplemental/10.1103/PhysRevB.102.035124> for a detailed discussion about the electrical resistivity and structural properties of materials considered in the main text, which includes Refs. [32–36].
 - [18] L. Nordheim, *Ann. Phys.* **401**, 607 (1931).
 - [19] P. Gegenwart, *Rep. Prog. Phys.* **79**, 114502 (2016).
 - [20] G. R. Stewart, *Rev. Mod. Phys.* **73**, 797 (2001).
 - [21] N. Nakashima, Y. Haga, E. Yamamoto, Y. Tokiwa, M. Hedo, Y. Uwatoko, R. Settai, and Y. Onuki, *J. Phys. Condens. Matter* **15**, S2007 (2003).
 - [22] E. C. Stoner, *Proc. R. Soc. London Ser. A* **165**, 372 (1938).
 - [23] D. Aoki and J. Flouquet, *J. Phys. Soc. Jpn.* **81**, 011003 (2012).
 - [24] U. Killer, W.W. Kim, A. Mielke, G. Fraunberger, J. J. Rieger, E. W. Scheidt, and G. R. Stewart, *Phys. Rev. B* **49**, 1188 (1994).
 - [25] M. Kang, N. Wakeham, Ni Ni, E. D. Bauer, J. Kim, and F. Ronning, *J. Phys.: Condens. Matter* **27**, 365702 (2015).
 - [26] R. B. Griffiths, *Phys. Rev. Lett.* **23**, 17 (1969).

- [27] H. Ikeda, in *Magnetism in Metals: A Symposium in Memory of Allan Mackintosh*, edited by D. F. McMorrow, J. Jensen, and H. M. Rønnow (The Royal Danish Academy of Sciences and Letters, Copenhagen, 1997), p. 359–374.
- [28] A. H. Castro Neto, G. Castilla, and B. A. Jones, *Phys. Rev. Lett.* **81**, 3531 (1998).
- [29] T. Vojta, *J. Low Temp. Phys.* **161**, 299 (2010).
- [30] V. Dobrosavljevic and E. Miranda, *Phys. Rev. Lett.* **94**, 187203 (2005).
- [31] D. Nozadze and T. Vojta, *Euro. Phys. Lett.* **95**, 57010 (2011).
- [32] E. Jobiliong, J. S. Brooks, E. S. Choi, H. Lee, and Z. Fisk, *Phys. Rev. B* **72**, 104428 (2005).
- [33] H. Yamada and S. Takada, *Prog. Theor. Phys.* **52**, 1077 (1974).
- [34] J. Pospíšil, M. Míšek, M. Diviš, M. Dušek, F. R. de Boer, L. Havela, and J. Custers, *J. Alloys Compd.* **823**, 153485 (2020).
- [35] N. Tateiwa, S. Ikeda, Y. Haga, T. D. Matsuda, M. Nakashima, D. Aoki, R. Settai, and Y. Onuki, *J. Phys.: Conf. Series* **150**, 042206 (2009).
- [36] J. J. M. Franse *et al.*, in *Physics of Solids under High Pressure*, edited by J. S. Schilling and R. N. Shelton (North-Holland, Amsterdam, 1981), p. 181.